Numerical simulation of the cathodic protection of pipeline networks under various stray current interferences

L. Bortels & J. Deconinck
Department of Electrical Engineering (TW-ETEC), Vrije Universiteit Brussel, Belgium.

Abstract

A simulation software for the design and evaluation of the cathodic protection (CP) of underground pipeline networks is presented. The macroscopic model behind the software expresses Laplace's equation in a flat and homogeneous three-dimensional half-space (soil) and takes into account the non-negligible ohmic voltage drop along the pipes. The soil (external problem) and pipes (internal problem) are coupled with each other through the pipeline coating. For this coating, an advanced model has been developed that takes into account the local soil resistivity, the holiday ratio, the average holiday size, the coating thickness and the coating resistance.

The model is solved using a combination of the boundary element method (BEM) for the external problem and the finite element method (FEM) for the internal problem. Special 'pipe-elements' have been used to reduce the calculation time. Anodes and railway tracks are replaced with equivalent (half-)pipes having the same resistance-to-soil as the anode or track, allowing a straightforward and flexible integration of all components (pipes, anodes and tracks) in the same model. Finally, rectifiers, current drains, sub-stations, electric trains and others are modelled as equivalent electrical networks that can connect any two points of the total configuration.

As a result, the model gives the 'on' and 'off' potential along the pipe, the potential distribution in the soil, the axial currents flowing through the pipes as well as the radial current densities leaving or entering the pipe walls. The software can deal with all standard kinds of cathodic protection interferences as well as stray currents coming from other CP-installations, DC-traction systems, HVDC-transmission lines, grounding systems and others.

WIT Transactions on State of the Art in Science and Engineering, Vol 7, © 2005 WIT Press
www.witpress.com, ISSN 1755-8336 (on-line)
doi:10.2495/1-85312-889-9/08

1 Introduction

Failures in oil or gas pipelines can have severe environmental and economic consequences. Therefore, large investments have been made in studies on corrosion prevention for buried pipes. Important research is being conducted to determine and predict the corrosiveness of the soil, corrosion mechanisms in the ground and effective protection techniques such as coating and painting of menaced metallic structures. Moreover, because of the hidden character of pipelines and their low accessibility, installation, survey, maintenance and repair is intricate, elaborate and expensive.

Numerical modelling can provide some relief by simplifying and optimizing installation, maintenance and repair. When used in the planning phase, conceptual mistakes can already be traced before any actual installation, by calculating different set-ups in cheap, harmless and fast simulations. Also, a model can provide reference values for measurements on operational sites, that can help in the tracing and solving of any possible anomaly. Last but not least, the model technique creates a safe and cost effective on screen 'virtual' test environment where new corrosion engineers can gain experience without long and expensive 'trial and error' experiments on site.

The fundamentals of such a mathematical model have been developed by F. Brichau, J. Deconinck and T. Driesens [1, 2]. Recently, ElSyCa developed CatPro [3], a PC-version of the code with windowing user-interface. (ElSyCa is a spin-off company of the Vrije Universiteit Brussel, developing simulation software in the field of electrochemistry and cathodic protection.)

The basic ideas and all fundamental aspects of the model are explained here. Mathematical details and the validation of the basic model have been discussed in detail in papers [1, 2].

2 Design of CP-systems : 'on' and 'off' pipe-to-soil potentials

When designing a cathodic protection system, the aim is to obtain a pipe-to-soil potential along the developed length of the pipeline network that is more negative than a certain minimum protection level. In soils, this minimum level is normally taken at $-0.85\mathrm{V}$ versus a copper-sulphate reference electrode (CSE) that needs to be placed directly adjacent to the pipeline in order to reduce the IR-drop in the soil and over the coating. The value obtained in this situation is referred to as the 'off' potential.

In practice however, due to the hidden character of the pipeline, it is often not possible to put the reference electrode directly near the pipeline. Instead, the reference electrode is put at the soil surface, directly above the pipeline which can result in important IR-drop errors. The value obtained here is referred to as the 'on' potential. In normal operating conditions, this value is more negative than the (true) 'off' potential, resulting in an overestimate of the obtained protection level.

In the following section, the mathematical model will be introduced. It will be demonstrated that both the 'on' and 'off' potentials can be calculated giving valuable

information on the obtained protection levels of the CP-configuration, even in very complex interference situations.

3 The mathematical model coupling BEM and FEM

In order to describe properly vast buried pipeline structures, one of the basic ideas of the model is to link the 'external' world – the soil – with the 'internal' world being the metallic conductor of the pipe (see fig. 1).

3.1 Soil and pipes – the external domain

The soil together with the pipes and anodes, being also a kind of pipes, is to be considered as an electrical/electrochemical system in which the earth acts as an electrolytic solution (conducting medium) and the outer metallic pipe surfaces are electrodes. If no ion concentration gradients are considered in the soil, Ohm's law applies and the current density J follows from:

$$\vec{J} = -\sigma\vec{\nabla}U, \tag{1}$$

where U is the potential, σ is the electrical conductivity of the soil and $\vec{\nabla}U$ is the electric field. When the conductivity of the soil is supposed to be uniform, the potential distribution in the soil is described by the Laplace equation, expressing conservation of charge:

$$\vec{\nabla}\cdot\left(\vec{\nabla}U\right) = 0. \tag{2}$$

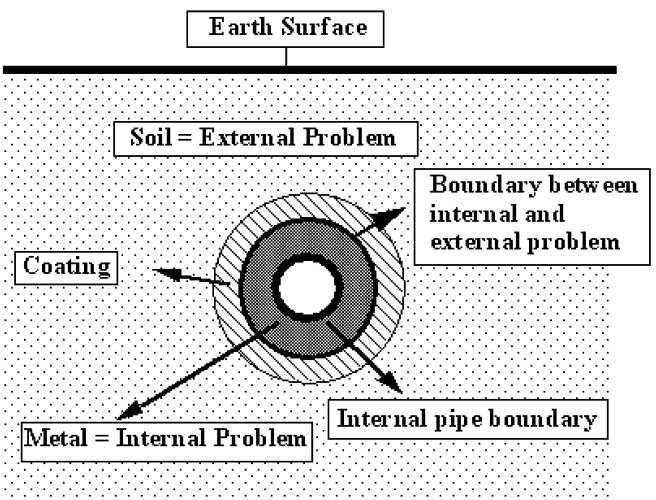

Figure 1: Cross section of a buried pipeline.

Do remark that at the earth surface (insulating boundary) the current density normal to the boundary is zero.

Because of the complex geometries found in practice and the non-linear boundary conditions, the Finite Element Method (FEM) and the Boundary Element Method (BEM) [4] have been the most successful numerical techniques to solve Laplace problems. However, there are strong arguments for using BEM to model underground corrosion. First of all, BEM is intrinsically well suited for infinite problems, since only the inner boundaries are to be defined with the infinite border implemented inherently. Further, assuming a perfectly flat earth surface, based on the so-called 'mirror-point' technique, the earth surface needs not to be discretised. Last but not least, the Boundary Element Method provides directly the local current densities on the metal surfaces, responsible for the corrosion.

3.1.1 Introduction of pipe elements

Because of the specific cylindrical shape of pipelines, special 'pipe elements' are used to perform the discretisation. These elements suppose a uniform, radial current density distribution. From a numerical point of view, this considerably reduces the problem description, since data input is based on outer pipe diameters and pipe lengths while elaborate element meshing is avoided. When one studies the error involved by assuming a uniform radial current density, it appears that the use of these pipe elements is justified, except when the configuration is bare and narrow, when coating holidays appear or when it is very close to another structure. Consequently, these hypotheses are not a true restriction in most cases encountered in reality.

In the same way, anodes will be replaced with a cylindrical rod having the same resistance-to-earth as the original groundbed as will be outlined in section (5.1). In fact formula, giving the resistance of a specific groundbed, usually are derived by making very similar assumptions.

3.2 Metallic pipes – the internal domain

For vast underground pipe structures the resistivity of the pipes in axial direction is no longer negligible. For a given pipe segment, the radial current coupled with the external world, enters and leaves the outer pipe surface (through the coating) while the collected axial current changes and causes a potential drop. The potential drop ΔV across a pipe segment with length L can be described using the following mathematical expression:

$$\Delta V = R_p \left\{ I_{ax} + \int_0^L J dS \right\}, \tag{3}$$

in which V is the potential of the metallic part of the pipe, R_p the resistance of the pipe segment, I_{ax} the collected axial current and J the radial current density.

3.3 Coupling between external and internal world

The coupling between the external problem (U) and the internal problem (V) is

simply achieved by expressing the boundary condition on the external surface of each pipe segment giving:

$$V - U = \eta(J_b) + RJ + E_{corr}, \tag{4}$$

in which U is the potential in the soil adjacent to the pipe, $\eta(J_b)$ is the pipe polarisation, RJ is the voltage drop across the applied coating (if any) and E_{corr} is the corrosion potential of the metal-soil system. The relation between the 'macroscopic' current density J and the current density J_b through the bare steel is given by:

$$J = \theta J_b, \tag{5}$$

in which θ represents the fraction of bare steel.

3.3.1 Polarisation of bare steel

The relation between the pipe polarisation and bare steel current density as used here is based on the work done by Orazem *et al* [5, 6]. They developed a fundamental expression for the electrochemical reactions that can occur on bare steel. An overview of the reactions that have been included in this work, together with the derived mathematical expression for the (partial) current density of that reaction, is given below:

- oxidation of metal : $Fe \rightarrow Fe^{2+} + 2e^-$

$$J_1 = 10^{(\eta^* - E_{Fe})/\beta_{Fe}}, \tag{6}$$

- reduction of oxygen : $O_2 + 2H_2O + 4e^- \rightarrow 4OH^-$

$$J_2 = -\frac{1}{\frac{1}{-J_{lim,O_2}} + 10^{(\eta^* - E_{O_2})/\beta_{O_2}}}, \tag{7}$$

- hydrogen evolution : $2H_2O + 2e^- \rightarrow H_2 + 2OH^-$

$$J_3 = -10^{-(\eta^* - E_{H_2})/\beta_{H_2}}, \tag{8}$$

with all parameters as explained below:

- $\eta^* = V - U^*$, the polarisation of bare steel,
- V the potential of the metallic part of the pipe,
- U^* the potential near the pipe just under the coating,
- J_1, the partial current density due to metal oxidation,
- E_{Fe}, the 'effective' equilibrium potential of Fe-reaction including the effect of the exchange current density,
- β_{Fe}, the Tafel slope for the Fe-reaction,
- J_2, the partial current density due to oxygen reduction,
- E_{O_2}, the 'effective' equilibrium potential of O_2-reaction including the effect of the exchange current density,

- β_{O_2}, the Tafel slope for the O_2-reaction,
- J_{lim,O_2}, the mass transfer limited current density for the O_2-reaction,
- J_3, the partial current density due to hydrogen evolution,
- E_{H_2}, the 'effective' equilibrium potential of H_2-reaction including the effect of the exchange current density,
- β_{H_2}, the Tafel slope for the H_2-reaction,

The total current density is given by:

$$J_b = J_1 + J_2 + J_3 = g(\eta^*), \tag{9}$$

a strong non-linear function of η^*. Remark that formula (9) is not relative to the corrosion potential E_{corr}. The corrosion potential is that value for η^* that is obtained when the current density, calculated using equation (9), is zero.

3.3.2 Coating quality

The potential drop across the coating is given by the relation:

$$U^* - U = RJ, \tag{10}$$

with:

- U the potential in the soil adjacent to the pipe,
- R the coating resistance.

The model for the coating as used here describes a perfect coating (no holidays) with a number of distributed holidays. All holidays are supposed to be cylindrical, with the same height as the coating thickness and with the same (average) diameter. In addition, it is assumed that these cylindrical holidays are filled with soil. According to literature [7], the resistivity of the holiday in first approximation is equal to about 10% of the surrounding soil resistivity.

The parameters for the coating resistance as described above are listed below:

- coating thickness,
- coating resistance,
- holiday fraction,
- resistance of holiday (as a fraction of local soil resistivity),
- average holiday diameter.

Based on these parameters and the local soil resistivity, the total coating resistance R can be calculated. Do remark that in the current model, the soil resistivity can be specified for each individual segment of the pipeline network.

3.3.3 Outcome of the calculations

Due to the coupling of internal and external domains the boundary conditions are only to be applied on the metallic structures (anodes and pipes). Either the total currents entering and leaving the whole system at given points, or the potential difference(s) between two or more points of the structure, or combinations of both are imposed. The general approach allows to deal in a straight forward way with two or more non intentionally connected metallic structures. They are anyway coupled via the earth.

As a consequence, the software provides all data of interest from a corrosion point of view:

- the 'off' potential in all points of the pipeline, by calculating the voltage difference between the (steel) pipe and the underside of the coating just above the steel,
- the 'on' potential in all points of the pipeline, by calculating the voltage difference between the (steel) pipe and the soil at surface level just above the pipeline,
- the axial currents flowing through the pipeline walls,
- the radial current densities entering or leaving the pipeline surfaces.

In addition, the ground resistivity, metal resistivity and geometrical aspects of the pipelines and anode beds, polarisation characteristics of the metallic surfaces, coating resistivity as well as imposed voltages and/or currents, joints, insulating joints and current drains are considered.

4 Modelling stray currents

In practice, stray currents play a non-negligible role in many underground cathodic protection problems. With respect to a given structure, a stray current is to be defined as a current flowing on a structure that is not part of the intended electrical circuit. For corrosion to occur as the result of stray currents, there must be an exchange of current between a metallic structure and an electrolytic environment. Due to stray currents, interference occurs.

Sources of stray currents are manifold. Some are caused by other cathodic protection installations, grounding systems, welding posts (and others), referred to as steady state stray currents. But most often traction systems like railroads and tramlines are responsible for large dynamic stray currents. As a result, also the prevention techniques for pipelines are numerous going from painting and coating to traditional cathodic protection and current drainage.

Similar to conventional corrosion prevention, all these methods reduce the stray current without increasing the anodic current density. Otherwise, high local anodic currents would cause rapid failure. In what follows these aspects will be considered in more detail.

4.1 Steady state stray currents

Because of the general fundamentals of the model, stray current problems involving different cathodic protection systems – with current or voltage controlled groundbeds – can be simulated without any preliminary extension. Even stray currents arising from grounded systems, like welding installations, may be calculated. The influence of distinct cathodic protection systems on each other appear automatically.

The well-known phenomenon of protection currents that bring about stray current corrosion in neighbouring bodies is called 'interference'. According to the kind and origin of the potential variations that come into play (cathodic or anodic), a distinction is made between cathodic, anodic, combined and induced interference. They all arise in a natural way in the model.

4.2 Dynamic stray currents

The initial approach of the underground model was exclusively based on buried cylindrical structures. In order to quantify stray-currents coming from traction systems, these traction systems are also to be modelled. This means that the rails and the above ground part containing sub-stations, overhead wires and trains are to be considered.

For reasons of logics and efficiency, the overhead network is considered as a separated electrical network, consisting of conductors, characterised by finite axial resistivity (lifelines, etc.) and node potentials (at sub-stations, trains, etc.) but with infinite radial resistivity since no current can leave the wire through the air. In this way, from the mathematical point of view, the overhead network is treated in just the same way as the internal pipe problem.

On the other hand, the rails have an axial and a radial resistivity, such that current can flow to and from the soil. A traction current that leaves the rails becomes a stray current that can enter a protected system. This means that, from the electrical point of view, there is nearly no difference between the buried pipelines and the rails at the earth surface.

4.3 Introduction of 'rail-pipes'

Although the shape of the rails together with bed and sleepers is not cylindrical, an equivalent semi-cylindrical 'pipe' can be defined that is a fairly good approximation, certainly at some distance from it. The axial resistivity is that of the rails and the radial resistivity corresponds to the resistivity found between rails and ground (details are found in section 5.2). So, in accordance with the standard definition of pipe elements in the model, the tracks are represented as equivalent pipes ('rail-pipes'). Their axis coincides with the earth surface and they are only in contact with the ground with their lower half. The axial 'rail-pipe' current equals that part of the traction current that directly returns to the sub-station. As the rail-pipes are coupled with the earth, the radial current densities can become stray currents when they are picked up by structures.

The 'rail-pipes' are coupled with the overhead network through the sub-stations. A given voltage difference is imposed between both. Finally, trains act as loads between overhead wires and 'rail-pipes'. They can be put on any place and the different traction modes can be simulated by varying the voltage (emf) and resistance of the load. All this has been indicated in figs 2 and 3.

This uniform approach makes the data entry very transparent and straightforward. The identification of the different types of involved rails, overhead wires, sub-stations, buried pipelines and protection systems can be based on their specific spatial and/or electrical characteristics.

5 Converting anodes and tracks into equivalent pipe elements

As mentioned before in sections (3.1.1) and (4.3), special 'pipe elements' are used to describe all pipes, anodes and tracks in the CP-configuration. Pipe elements have

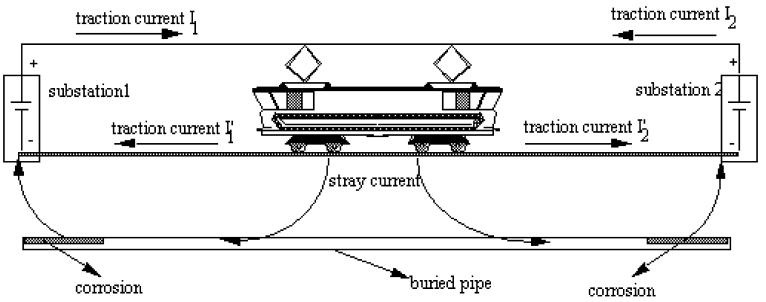

Figure 2: Traditional stray current situation for a railway.

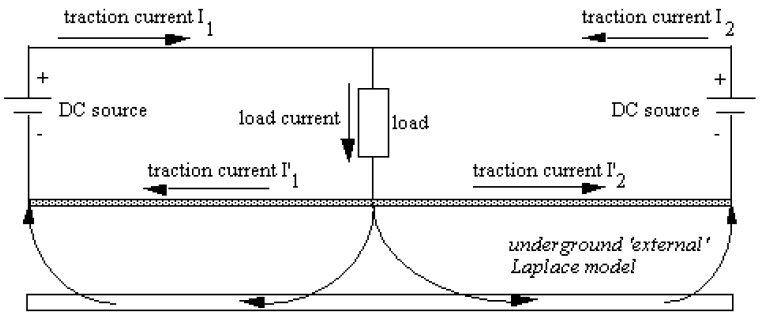

Figure 3: Equivalent electrical network used in the software.

uniform radial properties (current density, potential, ...) and are described by their outer diameter, inner diameter (or wall thickness) and axial resistivity.

For pipes, due to their intrinsic cylindrical shape, these data are directly available and no transformation formulas are needed. Anodes and tracks on the other hand can have shapes that are far from the *ideal* cylindrical shape. Therefore, special transformation formula are applied to obtain the equivalent 'pipe element'.

5.1 Converting an anode into an equivalent pipe element

Except when near anode details are needed, any anode bed can be replaced by an equivalent vertically buried full rod that has the same earth resistance as the original anode bed. For a full rod ($D_{out} = D, D_{in} = 0$), this resistance R is given by the well-known formula:

$$R = \frac{\rho_{soil}}{2.\pi.L} \ln\left[\frac{4L}{D}\right], \tag{11}$$

with L the length of the rod, D the diameter of the rod and ρ_{soil} the soil resistivity. The use of this formula is justified if $L \gg D$ and if there are no other electrodes in a region $< 5L$.

When doing numerical calculations, the anode with length L is divided into a number of calculation elements. The minimum length L_{min} of such an element is bounded by the condition:

$$L_{min} > 3D, \tag{12}$$

as outlined in the work of Modjtahedi *et al* [8]. Indeed, too small elements can cause oscillations in the calculated potential distribution along the anode. The non-linear equation (11) can be simplified by introducing a direct relation between L and D as given below:

$$L = kD, \tag{13}$$

with $k \gg 1$ in order to obey relation (12).

Combining equations (11) and (13) finally gives the length L of the equivalent anode element as a function of the resistance:

$$L = \frac{\rho_{soil}.\ln(4k)}{2.\pi}.\frac{1}{R}. \tag{14}$$

To conclude, the equivalent resistance R of the anode bed is obtained by dividing the measured anode potential (measured with respect to the far field) V_a and the rectifier current I:

$$R = \frac{V_a}{I}. \tag{15}$$

5.2 Converting a track into an equivalent pipe element

As outlined before in section (4.2), a track has to be replaced by an equivalent semi-cylindrical 'pipe element'. The original couple of rails that form the track have cross-section S. Common practice is to set the outer diameter D_{out} of the equivalent half-pipe equal to the distance d_{rails} between the center of the axes of both rails:

$$D_{out} = d_{rails}. \tag{16}$$

The inner diameter D_{in} is found by expressing that the cross-section of the equivalent half-pipe equals that of both rails:

$$\frac{\pi[D_{out}^2 - D_{in}^2]}{8} = 2S, \tag{17}$$

or in other words:

$$D_{in} = \sqrt{D_{out}^2 - 16\frac{S}{\pi}} \tag{18}$$

The axial resistivity ρ of the equivalent half-pipe is of course equal to that of the rails (assuming that both rails are made out of the same material).

6 Example 1: a simple pipe-anode configuration

The first example investigates the cathodic protection of a simple pipe-anode configuration.

6.1 Overview of the problem

Consider the problem of fig. 4. A coated steel pipeline buried at 5m depth receives cathodic protection from a long line zinc anode lying at the same depth by means of an impressed current system ($CS1$). The soil resistivity is $100\Omega.\mathrm{m}$.

The pipe has an outer diameter of 50cm, a wall thickness of 1cm and a coating with an average resistance of $220\Omega.\mathrm{m}^2$ and holiday ratio of 1%. The polarisation curve for bare steel has been taken from literature [6] and is presented in fig. 5 (with respect to the corrosion potential being $-0.56\mathrm{V}$ versus CSE). The anode is a solid cylindrical rod with a diameter of 10cm and an equivalent 'polarisation resistance' of $1\Omega.\mathrm{m}^2$. The corrosion potential is $-1\mathrm{V}$. Both the pipe and anode have a length of 100m.

6.2 Calculated 'on' and 'off' potentials

The calculated 'on' and 'off' potential are presented in fig. 6. As expected, the 'on' potential predicts higher protection levels than actually achieved along the pipeline. This is due to the additional effect of the IR-drop in the soil and across the coating which has not been eliminated (do remark that for the 'on' potential calculation the reference electrode is placed at the soil surface with all rectifiers on).

The error made when considering the 'on' potential as the protection criterion instead of the 'off' potential is about 177mV! The voltage drop across the coating

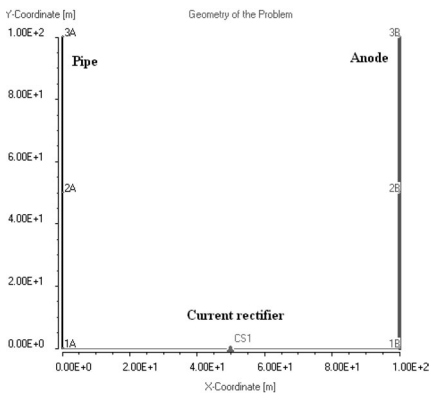

Figure 4: Geometry of the pipe-anode configuration (top view).

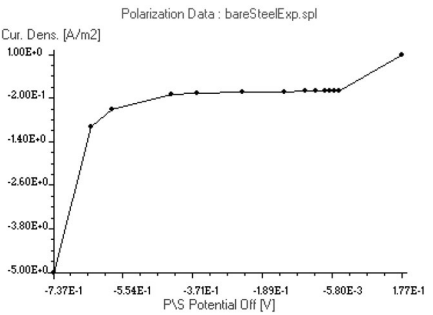

Figure 5: Polarisation curve of bare steel (relative to E_{corr}).

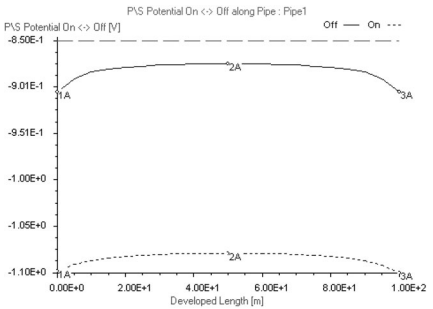

Figure 6: 'On' and 'off' potential along the pipe.

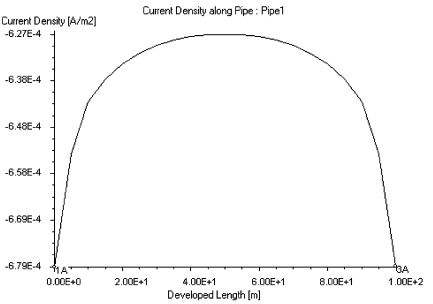

Figure 7: Radial current density along the pipe.

(current density multiplied with coating resistance) is about 147mV while that in the soil is about 30mV. A plot of the current density is presented in fig. 7. It must be mentioned that, since the fraction of bare steel is 1%, the 'macroscopic' current density J presented here is 100 times smaller than the actual polarisation current.

6.3 Potential distribution in the soil

The soil potential distribution in the neighbourhood of the pipe-anode system has been calculated on a raster with corners $(-50.0,-50.0,0.0)$ and $(150.0,150.0,0.0)$, and 31 points in both directions. The potential isolines calculated at earth level are presented in fig. 8. A maximum potential level of 69.2mV is obtained in the centre above the anode.

Similar results can be found by calculating the soil potential along a cutting line. This line goes from point $(-50.0,50.0,0.0)$ to point $(150.0,50.0,0.0)$, resulting in the soil potential distribution at earth surface level above the centre of the pipe-anode system. Results are shown in fig. 9. The same minimum and maximum values for the soil potential as before are found.

7 Example 2: a parallel pipeline configuration

In this example it will be demonstrated how the software can be used to study the interference between two parallel pipelines having different coating properties. It is shown how a single groundbed can be used to protect multiple pipelines. Finally, it is demonstrated how experimental data for the soil resistivity along the pipeline(s) can be used as input for the numerical calculations.

7.1 Overview of the problem

The idea behind this example is partly based on the paper of Carlson *et al* [9]. A new $36''$ pipeline (referred to as 'Main Pipe' or 'New Pipe') with a total length of 84km is coated with fusion-bonded epoxy (FBE). Along its total length, it runs parallel to an older $24''$ pipeline ('Secondary Pipe' or 'Old Pipe') at a constant distance of 20m.

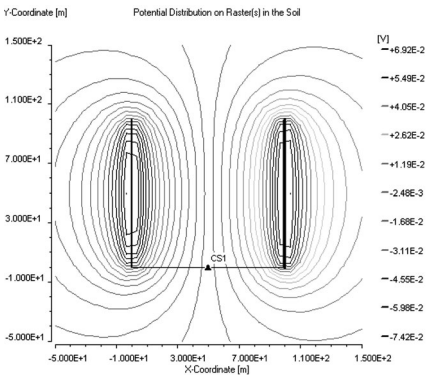

Figure 8: Soil potential distribution in the vicinity of the pipe-anode system.

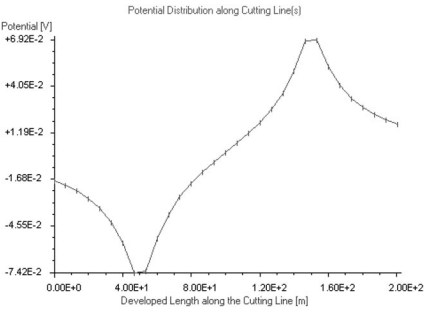

Figure 9: Soil potential distribution above the centre of the pipe-anode system.

The centre of both pipes is located at a constant depth of 1.5m. The average soil resistivity along the pipeline trajectory is 20Ω.m.

The polarisation behaviour for both pipes is described by a non-linear polarisation curve that takes into account metal oxidation and oxygen and water reduction. The corrosion potential for the new and old pipe is $-0.656\mathrm{V}$ and $-0.704\mathrm{V}$, respectively (versus CSE).

The model for the coating quality used for both pipes describes a perfect coating (no holidays) with a number of distributed holidays. The holiday ratio is 0.005% for the new pipeline and 0.1% for the old one. Taking into account a soil resistivity of 20Ω.m, this yields a coating resistance of about $31300\Omega.\mathrm{m}^2$ and $1570\Omega.\mathrm{m}^2$, respectively.

7.2 Cathodic protection design analysis

Based on the soil resistivity and coating quality data as specified in the previous section, an average current density distribution of $1.25\ 10^{-5}\mathrm{A}/\mathrm{m}^2$ for the new pipeline is taken. This results in a current requirement of 35.9mA/km or about 3A in total.

For the old pipe, having a coating resistance that is about 20 times lower than that of the main pipe, an average design current density of $2.2\ 10^{-4}\mathrm{A}/\mathrm{m}^2$ is taken. Hence, the old pipe requires a current value of 420.2mA/km or about 35A in total.

As outlined in the work of Carlson *et al* [9], and taking into account the assumed coating quality as described above, the groundbed spacing for the new pipeline is about 30km. With the total length of the pipe being 84km, the minimal number of groundbeds to ensure a smooth voltage profile is 3, resulting in a final spacing of 28km. In terms of developed length, this means that groundbeds should be placed at 14, 42 and 70km. Since the total current requirement for the main pipeline is 3A, a current output of 1A per groundbed is needed.

For the old pipeline, having an inferior coating and hence an increased attenuation, an extra groundbed in-between two successive groundbeds is placed (at $7, 28, 56$ and 77km). This means that for the old pipe in total 7 groundbeds are used, each delivering a current output of 5A. Do remark that for the old pipe, to be fully 'correct', the 7 groundbeds should be placed with a spacing of 12km and not 14km as it is now (resulting in a smaller spacing and hence a higher protection level at begin and end).

In this example, we will use deep-anode groundbeds, located at a depth of 70m and at a horizontal distance of 10m with respect to the pipe. The resistance-to-ground of the anode beds is 1Ω.

An overview of the pipeline geometry and rectifier location is given in fig. 10.

7.3 Results

First of all, one will verify the design of each pipeline separately. Finally, the complete CP-configuration and the interference between both pipes will be investigated.

7.3.1 Study of the CP of the main pipeline

What we are interested in, is the 'off' potential along the developed length of the pipeline. As can be seen from fig. 11, the design as outlined above gives a very smooth distribution with pipe-to-soil values ranging between -0.90 and -0.91V. Figure 12 gives a comparison between the 'on' and 'off' potentials. The IR-drop error made when considering the 'on' potential is around 410mV.

From the solver output presented in fig. 13 and the current density profile from fig. 14, it can be noted that for a current output of 1A per anode, the average current density along the pipeline matches the designed value (see 7.2).

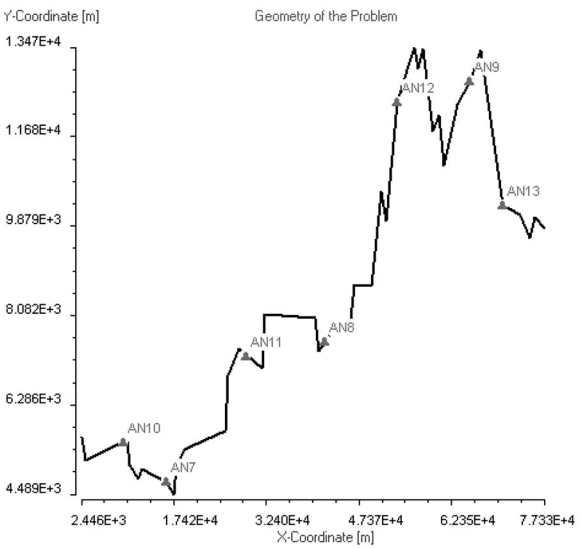

Figure 10: Position of the rectifiers along the pipelines (top view).

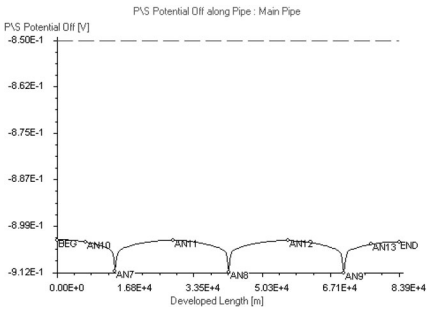

Figure 11: 'Off' potential for the main pipeline.

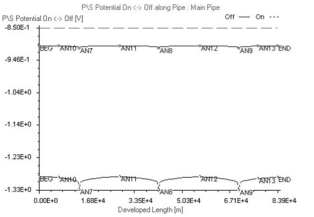

Figure 12: Comparison between 'on' and 'off' potential (main pipeline).

7.3.2 Study of the CP of the secondary pipeline

As outlined before, the secondary pipeline is protected using 7 groundbeds, each delivering a current output of 5A and with the labels for the rectifiers being AN7 to AN13.

As can be seen from fig. 15, the design as outlined above again gives a smooth distribution with 'off' values ranging between -0.92 and -0.95V. The calculated 'on' potentials are again much more negative than the corresponding 'off' potentials (fig. 16). The highest IR-drop (555mV) is found near groundbed AN13, the lowest one (340mV) in the middle of AN8 and AN12.

However, when compared with the 'off' potentials of the main pipeline, it can be noticed that at the beginning and end of the pipeline, there is a slight 'overprotection' when compared with the rest of the pipeline. This effect is due to the groundbed location for the secondary pipeline which is not 'perfect' as already mentioned in section 7.2.

7.3.3 Study of the CP of both parallel pipelines

Do remark that for the parallel pipeline problem, groundbeds AN7 to AN9 will be used to protect both pipelines as can be seen from fig. 17. One side of the

```
############## Outgoing Current per Branch ###############

Main Pipe :   I = -3.000E+00[A] , J = -1.245E-05[A/m2]
Anode 7   :   I = +1.000E+00[A] , J = +1.061E+00[A/m2]
Anode 8   :   I = +1.000E+00[A] , J = +1.061E+00[A/m2]
Anode 9   :   I = +1.000E+00[A] , J = +1.061E+00[A/m2]
------------------------------------------------------------
Current Balance of All Branches     =     -1.408E-06 [A]

############################################################

Total Time needed for the Solution Process = 10 seconds
```

Figure 13: Solver output (main pipeline).

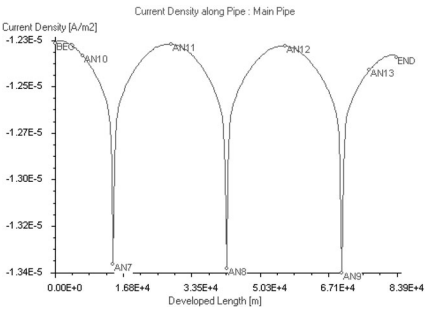

Figure 14: Current density (main pipeline).

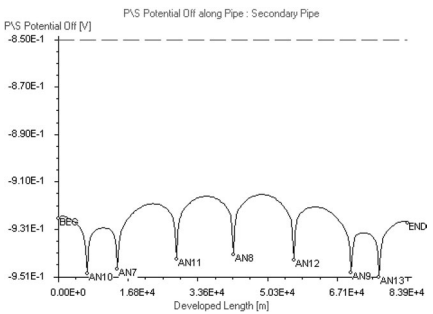

Figure 15: 'Off' potential for the secondary pipeline.

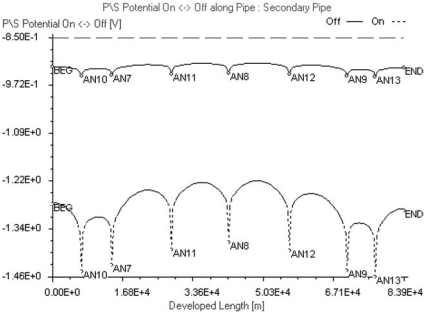

Figure 16: 'On' and 'off' potential for the secondary pipeline.

current rectifier is connected to the anode while the other side (split point − SP1) is connected to both pipelines using two different connections (JO1 and JO2). The total rectifier current (being $1\text{A} + 5\text{A} = 6\text{A}$) will be distributed between both pipelines depending on the coating resistance, polarisation and ohmic effects in pipes and soil.

As can be seen from the solver window (fig. 18), the total protection current for the main pipeline is 3.1A, 34.9A for the secondary pipeline and 38.0A in total. This means that, due to the rectifier connection of fig. 19 an additional current of 0.08A is used for the cathodic protection of the main pipe. Indeed, the currents flowing in the external connections of the main pipeline (fig. 19) at locations AN7 to AN9 are respectively equal to 1.3, 0.4 and 1.4A. The other part of the total current of 6.0A at those locations is consumed by the secondary pipeline as seen from fig. 20.

The 'off' potentials along both pipelines are presented in figs 21 and 22 and compared with those calculated from the separate configurations. As before, the distribution is rather smooth with peak values of -0.90 and -0.94V for the main pipeline and -0.92 and -0.95V for the secondary pipeline.

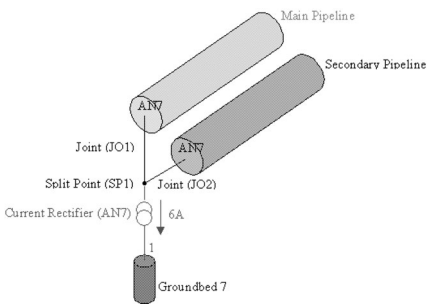

Figure 17: Protecting two pipelines using a single groundbed.

```
############## Outgoing Current per Branch ##############

Main Pipe      :  I = -3.079E+00[A] , J = -1.278E-05[A/m2]
Secondary Pipe :  I = -3.492E+01[A] , J = -2.175E-04[A/m2]
Anode 7        :  I = +6.000E+00[A] , J = +6.366E+00[A/m2]
Anode 8        :  I = +6.000E+00[A] , J = +6.366E+00[A/m2]
Anode 9        :  I = +6.000E+00[A] , J = +6.366E+00[A/m2]
Anode 10       :  I = +5.000E+00[A] , J = +5.305E+00[A/m2]
Anode 11       :  I = +5.000E+00[A] , J = +5.305E+00[A/m2]
Anode 12       :  I = +5.000E+00[A] , J = +5.305E+00[A/m2]
Anode 13       :  I = +5.000E+00[A] , J = +5.305E+00[A/m2]
-------------------------------------------------------
Current Balance of All Branches    =     -5.899E-04 [A]

#########################################################

Total Time needed for the Solution Process = 48 seconds
```

Figure 18: Solver output for the parallel pipeline configuration.

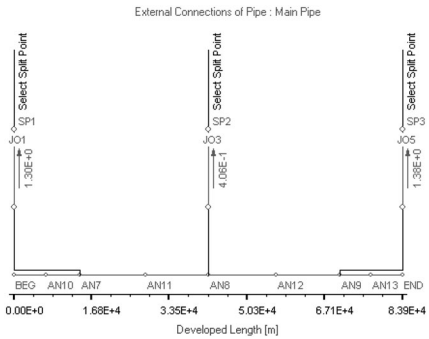

Figure 19: External connections for the main pipeline.

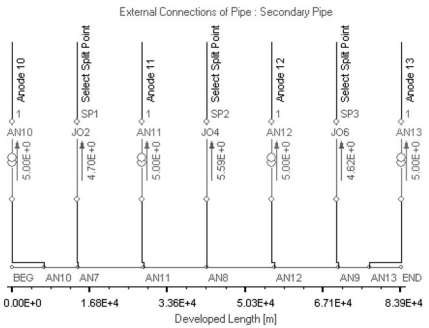

Figure 20: External connections for the secondary pipeline.

Do remark that the main pipeline gets an extra protection near the position of the additional four groundbeds of the secondary pipeline. This is not surprising since both pipelines are only 20m separated from each other.

From fig. 21 it can be seen that the average 'off' potential is only slightly more negative than before (except near groundbed AN8). This is due to the fact that the additional current of 0.08A is less than 3% of the original 3A. Similarly, the decrease of 0.08A in rectifier current for the secondary pipeline only gives a minor decrease in overall protection level as can clearly be seen from the results presented in fig. 22. Remark that near groundbed AN8, the protection level for the secondary pipeline is slightly better than in the isolated case.

7.4 Using experimental soil resistivity values as input

In practical situations, the soil resistivity along the trajectory of the pipeline is measured at a given number of intervals. These experimental resistivity data can directly be used within the calculations. An overview of such a file is given in fig. 23. Only a reduced number of data, 'measured' at the groundbed locations has

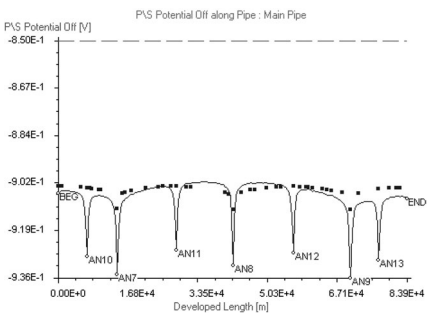

Figure 21: 'Off' potential along the main pipeline.

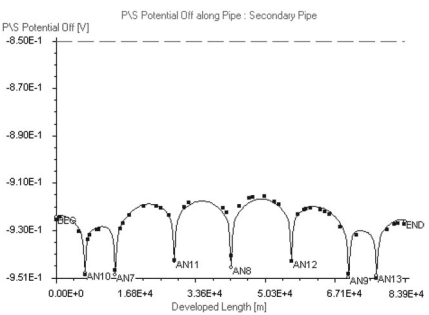

Figure 22: 'Off' potential along the secondary pipeline.

```
CatPro fieldfile version 1.3
2
7
L     RESIS
6966  20
14278 35
28457 50
42107 3
56602 5
70344 45
77102 60
```

Figure 23: Specifying the soil resistivity data for the main pipeline.

been entered. In between two successive data points, the soil resistivity is assumed to vary linearly.

The pipe-to-soil values along the main and secondary pipeline are presented in figs 24 and 25. The 'off' potential in the region between anodes 8 and 12 is more negative than before due to the reduced soil resistivity (ranging between 3 and $5\Omega.\mathrm{m}$) and hence and increased current density. The regions near groundbeds AN11 and AN13, exhibiting the highest soil resistivity, are no longer protected. The secondary pipeline remains protected over the full length of it.

Finally, the coating resistance along both pipelines is shown in figs 26 and 27. For the main pipeline, the resistance ranges from 4780 to $93400\Omega.\mathrm{m}^2$. The values for the secondary pipeline are about 20 times smaller.

8 Example 3: DC-traction stray currents influences

In this example it is explained how the software can be used to study DC-traction stray current influences on the cathodic protection of buried pipelines. This type of stray current is one of the most important sources of earth corrosion and generally results from the leakage of return currents from large DC-traction systems that are grounded or have a bad earth-insulated return path.

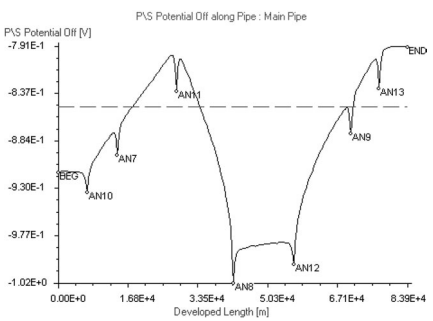

Figure 24: 'Off' potential for the main pipeline.

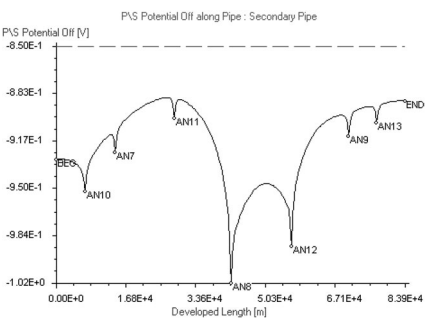

Figure 25: 'Off' potential for the secondary pipeline.

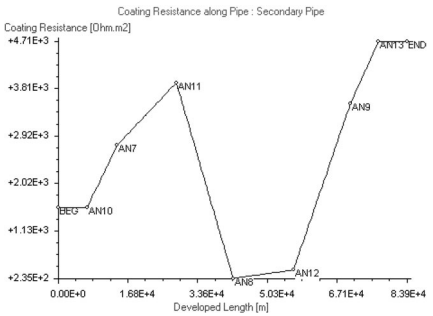

Figure 26: Coating resistance for the main pipeline.

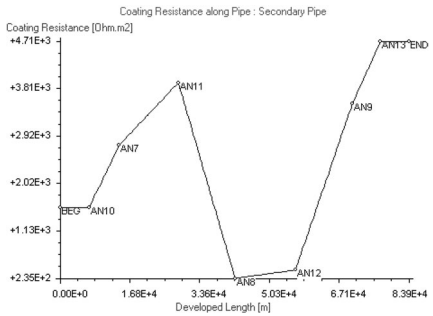

Figure 27: Coating resistance for the secondary pipeline.

The duration and the amplitude of the involved processes are important for the resulting metallic corrosion. Cathodic protection systems and railways rely for their function on large, persistent earth currents or suffer from periodic traffic, consuming substantial currents. Therefore the cathodic protection system becomes more complicated and has to be properly designed as will become clear from the calculations that follow.

8.1 Overview of the problem

Consider the practical situation of fig. 28. A large $30''$ gas transport pipeline with a total length of about $60\mathrm{km}$ is protected by two deep-anode groundbeds. The centre of the pipe is located at a constant depth of $1.5\mathrm{m}$. The average soil resistivity along the pipeline trajectory is $100.0\Omega.\mathrm{m}$. The groundbeds are at a depth of $20\mathrm{m}$ and a distance of $50\mathrm{m}$ with respect to the pipe.

On the left of the pipe, at a certain varying distance, lies a rail-road, composed out of two tracks, the first one crossing the pipeline. The power stations (sub-stations), indicated with PS1 to PS4, are at a distance of about $15\mathrm{km}$. It is evident that both tracks can be electrically connected in practice. This information is introduced by means of two joints JO1 and JO2, connecting both tracks and both overhead wires, respectively. Two trains (TR1,TR2), one on either track, are present. The polarisation behaviour for the pipe is described by the same non-linear polarisation curve as used for the old pipeline from the previous example (with a corrosion potential of $-0.7\mathrm{V}$).

The coating quality is again described using a perfect coating (no holidays) with a number of distributed holidays. The holiday ratio is 0.05% and the average defect size is 1cm. Taking into account a soil resistivity of $100\Omega.\mathrm{m}$, this yields a coating resistance of about $1610\Omega.\mathrm{m}^2$.

Anode beds CS1 and CS2 are of the impressed current type and deliver respectively 3.9A and 4.1A (at 13.8V and 14.9V). This yields a resistance-to-ground of the anodes being 3.53Ω and 3.63Ω. The sub-stations PS1 to PS4 deliver a voltage of 1500V and the load resistance representing the traction current is 1Ω for both trains. The transition resistance between track and soil is $10,000\Omega.\mathrm{m}^2$.

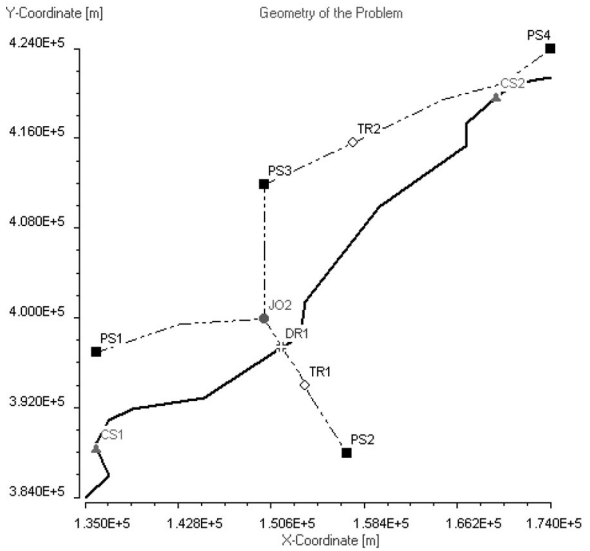

Figure 28: Simulation of DC-traction stray currents.

8.2 Simulation without trains

First, a simulation without trains is done. In fig. 29, the 'off' potential is plotted along the developed pipe length for the case with both anode beds operational. One can see that the entire pipeline is protected ('off' potential more negative than -0.85V versus CSE, see dashed red line) using only two anode beds.

A plot of the corresponding axial current along the pipeline is presented in fig. 30. This current is defined as being positive if it does flow in the direction from lower left to upper right on fig. 28. Negative values in fig. 30 therefore represent axial currents in the opposite direction. Note the two 'current jumps' at the position of the anode beds where respectively 3.9 and 4.1A are 'extracted' from the pipe.

8.3 Simulation with a train at position 1

Consider first train TR1 at position 1. The calculated 'off' potential is presented in fig. 31 and has been compared with the results from the stray current free simulation, presented in brown squares.

The train takes in total 1120A from the current feeder. This current is mainly delivered by sub-stations PS1 (172A), PS2 (733A) and PS3 (212A) and in less amount by PS4 (5.8A). The current returns to the sub-stations mainly via the rails. However, looking at the pipe-to-soil potential distribution along the pipeline in fig. 31, it appears that an important part of the current enters the pipe at the crossing with the rail. This effect induces locally a cathodic (over-)protection of the pipe that is even more important than the anode influences. This stray current reduces the local current density along some important parts of the pipeline.

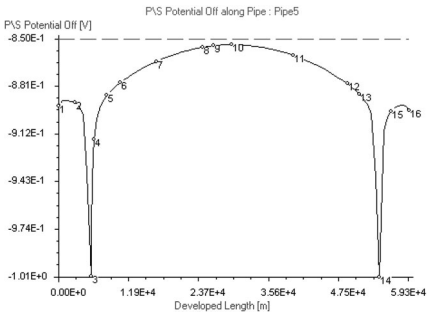

Figure 29: 'Off' potential (no trains).

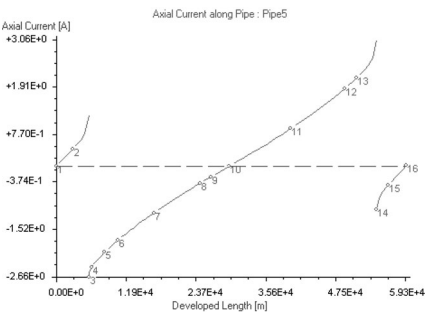

Figure 30: Axial current (no trains).

Indeed, near location 11, the 'off' potential drops to only -0.84V, a little bit below the minimum protection level! In the region near anode bed CS1, the protection level is slightly lowered (but still more negative than -0.85V versus CSE) and the stray current flows via the rails back to sub-stations PS1 and (in less amount) PS2.

To the north however, the stray current picked up at the crossing severely reduces the protection level of the pipe. The rail between PS3 and PS4 plays an important role and it can be observed that large parts of the pipeline are just below the minimum protection level. Fortunately, but not by chance, the position of anode bed CS2 considerably reduces the effect.

From fig. 32, comparing the calculated 'on' and 'off' potential, it can be seen that near the crossing the stray current produces an 'on' potential that is about 950-mV more negative than the true 'off' potential! The IR-drop along the coating can be calculated from the current density profile and the coating resistance. It turns out that the IR-drop along the coating is 515mV. The other 435mV potential drop is due to the soil between the pipe and the reference electrode at the earth surface.

8.3.1 Potentials along track and overhead wire

The stray current pattern generated by train TR1 strongly depends on the potential of the track, as shown in fig. 33.

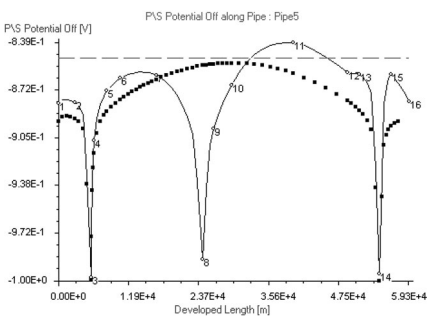

Figure 31: 'Off' potential (TR1 active).

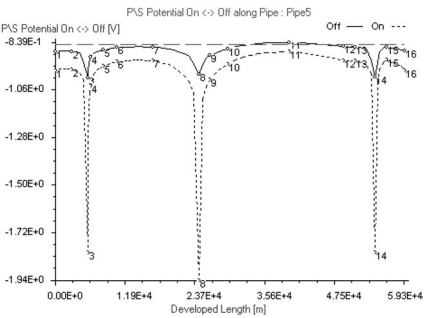

Figure 32: 'On' and 'off' potential (TR1 active).

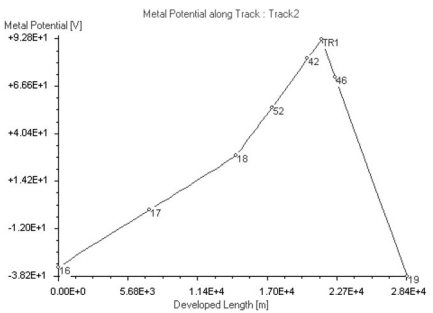

Figure 33: Track potential (TR1 active).

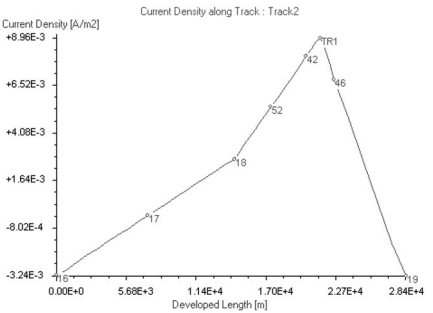

Figure 34: Track current density (TR1 active).

From this plot is can be seen that the highest track potential ($+92.8$V) is found-at the position of the train, and the lowest one near the sub-stations PS1 (-32.5V) and PS2 (-38.2V). Track regions at high voltages generate stray currents that leave the rail (positive current density) and return back to the track (negative current density) near the sub-stations as can be seen from the rail current density plot of fig. 34.

8.3.2 External network belonging to a track

A complete overview of the track-wire network with all external connections (trains, sub-stations, drains, joints, ...) is shown in fig. 35. From this figure it can be seen that the train indeed receives 1120A and that 182A flows to the other track through joint JO1. The overhead wire receives 217A, injected via joint JO2.

8.4 Simulation with a train at position 2

Next consider train TR2 at position 2 (TR1 being disabled). The train takes 1050A from the current feeder. This current is almost completely delivered by sub-stations PS3 (721A) and PS4 (321A) and returns mainly to the sub-stations via the rails. The corresponding pipe-to-soil potential along the pipeline is given in fig. 36.

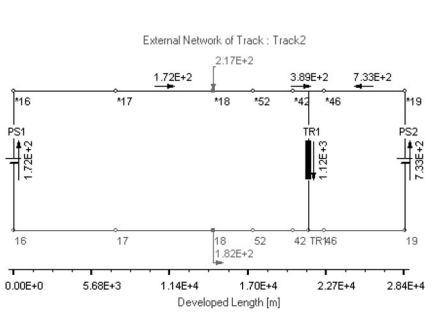

Figure 35: External network (TR1 active).

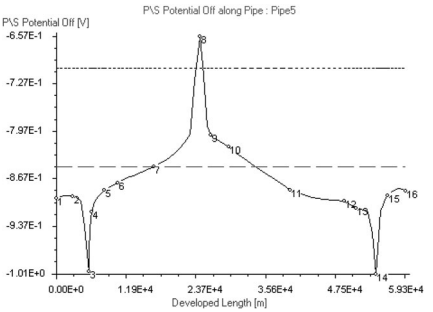

Figure 36: 'Off' potential (TR2 active).

An important part of the traction current leaves the pipe at the crossing with the rail and returns via the rail back to sub-station PS3. As a result the part of the pipe near the crossing is made anodic (pipe-to-soil potential higher than corrosion potential) and severe local corrosion occurs. The stray current enters the pipeline in the neighbourhood of anode bed CS2 where the distance between rail and pipe is small. The effect of the stray current is added to the effect of the anode bed CS2. Overprotection might take place. The region near to anode bed CS1 is scarcely influenced during this situation.

It is interesting to have a closer look at fig. 37, comparing the calculated 'on' and 'off' potential. One can clearly observe that in a zone near the crossing, the calculated 'on' potential is indeed less negative than the corresponding 'off' potential, clearly indicating that at this position, current leaves the pipeline and corrosion occurs. This is also confirmed by the current density profile presented in fig. 38.

8.5 Influence of a current drain at the crossing

When the sources of stray currents are accessible, current drainage techniques can be implemented. This means that the structure that suffers from stray current corrosion, being the pipe, is connected to the negative pole of the DC-source that generates the stray current (*i.e.* the first track). This metallic connection must have a lower resistance than the alternative earth return path.

Moreover, the current drain is made unidirectional (*i.e.* a diode in series with a resistance R), such that current can only flow from the pipe to the track. Stray currents that entered the pipe will then prefer this connection to return to the generator, instead of the soil. The amount of current that is drained from the pipeline can be controlled by changing the resistance R of the drainage.

In practice, such a unidirectional drainage is present at the crossing of the pipe and the track as can be seen from fig. 28 (DR 1). Simulations with R respectively equal to 10.0, 5.0 and 2.0Ω have been performed, resulting in a drain current of 2.0, 3.8 and 8.6A, respectively. From fig. 39 ($R = 5.0\Omega$) and fig. 40 ($R = 2.0\Omega$) it is clearly noticed that the drainage with the lowest resistance is working well,

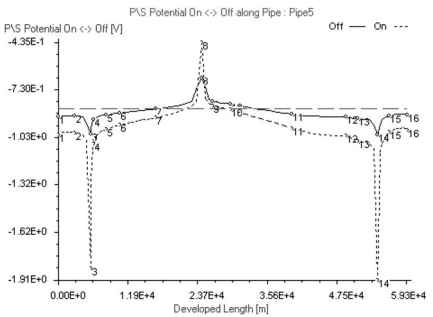

Figure 37: 'On' and 'off' potential (TR2 active).

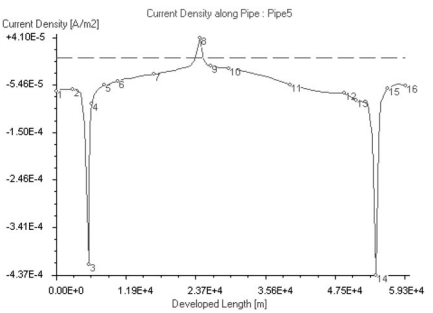

Figure 38: Current density (TR2 active).

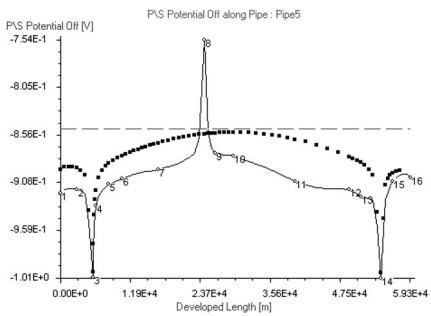

Figure 39: 'Off' potential (TR2 active drain resistance = 5Ω).

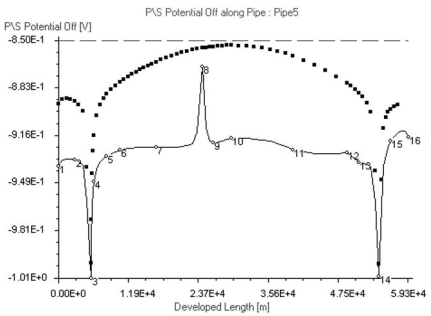

Figure 40: 'Off' potential (TR2 active drain resistance = 2Ω).

ensuring a protection of the pipeline along the whole length (squares represent stray current free simulations). Although not presented here, it turns out that a drain with negligible resistance R gives a protection level near the crossing of -1.04V, comparable to that near the groundbeds. The drain current in this case is about 53.5A.

8.6 Influence of the joint between the tracks and wires

As mentioned in the introduction of the problem, both tracks and overhead wires are connected to each other by means of joints JO1 and JO2, respectively. When both joints are active, the external networks associated with both tracks are, from an electrical point of view, fully coupled. In what follows, it will be investigated how the stray currents behave if one or both of the joints are inactive.

Let's first find out what happens to the stray current pattern produced by TR1 at position 1. Therefore, in total 4 calculations have been done with JO1 and JO2 switched on and off. An overview of the results found is presented in table 1. For each run, the currents through the joints (when active) and the sub-stations have been presented, followed by the pipe-to-soil potential (protection level) of the pipe at the crossing and at the end of the pipeline (point 15, just after anode bed CS2).

Joint JO1 has been defined from the first to second track. This means that a negative value in table 1 indicates a current that flows in the opposite direction. The same remark holds for joint JO2.

Table 1: Influence of JO1 and JO2 on the current balances (TR1 active).

case	JO1 [A]	JO2 [A]	PS1 [A]	PS2 [A]	PS3 [A]	PS4 [A]	PSP (8) [V]	PSP (15) [V]
on-on	182	-217	172	733	212	5.8	-0.99	-0.86
on-off	18.7	N.A.	268	813	1.8	-1.8	-0.96	-0.89
off-on	N.A.	-128	210	765	115	13.7	-1.03	-0.85
off-off	N.A.	N.A.	268	813	0.01	-0.01	-0.97	-0.89

From this table and the overview fig. 41, it can clearly be seen that the largest stray current at the crossing and the lowest protection level at the end of the line are obtained when JO2 is active and JO1 is inactive. In this case, the train still receives current from PS3 and PS4 since JO2 is active, explaining the large protection level (stray current pick-up) at the crossing. However, the return path for the traction current is partly blocked since JO1 is inactive, encouraging the current to go back to PS3 and PS4 via the pipe, and hence explaining the reduced protection level of the pipe between both sub-stations.

In fig. 42, all external connections associated with the second track are given in the case when JO1 is active and JO2 is not. From this figure and table 1 it can be seen that a current of 18.7A originates from the first track and enters the network through JO1. Part of this current (1.78A) goes through PS3 and circulates in the network between both sub-stations, other parts follow the track and leak into the soil. Remark that the metal potential of the track at PS3 and PS4 is 8.3V and 6.9V respectively with a minimum of 5.9V at the point nearest to the pipeline in the region of CS2.

A summary of the stray current patterns produced by TR2 at position 2 (TR1 and DR 1 are inactive) is presented in table 2. From this table and the overview fig. 43, it can be remarked that the influence of JO1 in this situation is almost completely negligible. When both joints are active the current through JO1 is only 25.4A compared to the 182A in the previous case (TR1 at position 1). Again, the largest stray current influences at both the crossing and at the end of the pipeline are obtained when JO1 and JO2 are both active.

8.7 Influence of unbalanced sub-station voltages

In the previous calculations, the influence of traction current leaks on the cathodic protection of the pipeline has been investigated. However, stray currents can also originate from DC-traction systems when no trains are present due to unbalanced

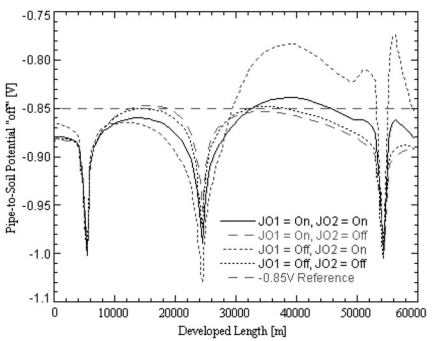

Figure 41: 'Off' potential for different modes of JO1 and JO2 (TR1 active).

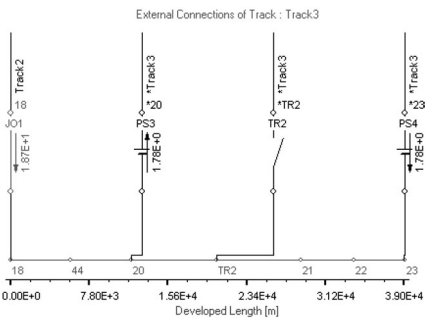

Figure 42: External connections associated with the second track (TR1, JO1 active; JO2 inactive).

Table 2: Influence of JO1 and JO2 on the current balances (TR2 active).

case	JO1 [A]	JO2 [A]	PS1 [A]	PS2 [A]	PS3 [A]	PS4 [A]	PSP (8) [V]	PSP (15) [V]
on-on	25.4	12.9	6.4	6.5	721	321	−0.66	−0.89
on-off	35.1	N.A.	0.1	−0.1	733	321	−0.66	−0.89
off-on	N.A.	25.1	12.3	12.7	708	322	−0.69	−0.88
off-off	N.A.	N.A.	0	0	729	324	−0.83	−0.88

sub-station voltages. To demonstrate this the voltage delivered by PS1 and PS2 will be increased with 5% and compared with the standard situation were all sub-stations are at 1500V. For each test case, the metal potential of the track at PS1 and PS2 has been noted. At the crossing, the protection level ('off' potential) of the pipe, the metal potential of the pipe and the metal potential of the track have been investigated.

An overview of the results is given in table 3. From this table it can be seen that when all sub-stations are perfectly balanced, the metal potential of the track at the crossing is very close to zero. However, when one of the sub-stations is out of balance, a continuous compensation current will flow between PS1 and PS2. The track potential at the sub-station that delivers the highest voltage will be the lowest, *i.e.* −18.5V in both cases. The worst case however is encountered when PS2 (being closer to the crossing than PS1) delivers the highest voltage (1575V). In this case, the metal potential of the track at the crossing with the pipe is the lowest (*i.e.* −5.35V), which will increase the discharge of current from the pipe at that position. Therefore the protection level of the pipe at the crossing drops to −0.78V, which is below the minimum value. An overview of the protection level of the whole pipeline in this situation is given in fig. 44.

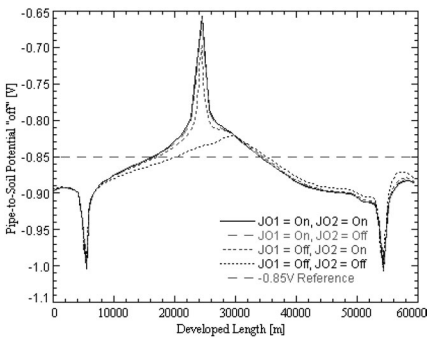

Figure 43: 'Off' potential for different operation modes of JO1 and JO2 (TR2 active).

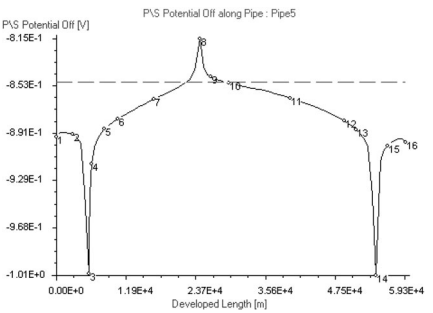

Figure 44: 'Off' potential (PS2 at 1575V).

Table 3: Influence of unbalanced voltages between PS1 and PS2 (no trains).

PS1 [V]	PS2 [V]	$V_{t,PS1}$ [V]	$V_{t,PS2}$ [V]	$V_{p,cross}$ [V]	$V_{t,cross}$ [V]	PSP_{cross} [V]
1500	1500	$+0.0$	$+0.0$	-0.87	$+0.0$	-0.86
1575	1500	-18.5	$+5.8$	-0.87	-0.24	-0.85
1500	1575	$+5.8$	-18.5	-0.87	-5.34	-0.78

9 Conclusion

A simulation software dedicated to the modelling of the cathodic protection of networks of buried pipeline has been presented. This model accurately deals with problems involving multiple cathodic protection systems. As a result, interference situations occurring when several CP-systems interact, can be calculated. It has been shown how the coupling with an additional aboveground electrical network and the introduction of special pipes, representing railways, allows to model stray currents arising from traction systems.

The extended model has been tested on underground corrosion situations involving parallel pipelines and traction systems. The dc-traction calculation clearly shows how stray current can have important influences at a long distance from their place of creation. Their impact on the overall protection level of the pipeline depends on several parameters such as the overall geometry, train positions, sub-station voltages, joints, ... The combined effect of all those influences makes it very difficult or even impossible to predict the outcome without a powerful simulation tool that can investigate all these influences. It has been proven that the developed model is a powerful, flexible and straightforward simulation tool that enables calculation of many real situations encountered in corrosion of underground pipelines.

References

[1] Brichau, F. & Deconinck, J., A numerical model for cathodic protection of buried pipes. *CORROSION*, **50(1)**, pp. 39–49, 1994.

[2] Brichau, F., Deconinck, J. & Driesens, T., Modeling of underground cathodic protection stray currents. *CORROSION*, **52(6)**, pp. 480–488, 1996.

[3] Catpro software manual, www.elsyca.com.

[4] Brebbia, C.A., Telles, J. & Wrobel, L., (eds.) *Boundary Element Techniques*. Springer-Verlag: Berlin and New York, 1984.

[5] Orazem, M., Esteban, J., Kennelley, K. & Degerstedt, R., Mathematical model for cathodic protection of an underground pipeline with coating holidays: Part 1 – theoretical development. *CORROSION*, **53(4)**, pp. 264–272, 1997.

[6] Orazem, M., Esteban, J., Kennelley, K. & Degerstedt, R., Mathematical model for cathodic protection of an underground pipeline with coating holidays: Part 2 – case studies of parallel anode cathodic protection systems. *CORROSION*, **53(6)**, pp. 427–436, 1997.

[7] Biase, L.D., Corrosione da corrente alternata su tubazioni metallische interrate: stato dell'arte e prospettive. *Convegno Nazionale APCE Roma*, 1996.
[8] Modjtahedi, D. & Jamali, M., BEM with fundamental sources placed on an imaginary boundary. *Proceedings of 12th International Conference on Boundary Elements Method*, pp. 111–121, 1990.
[9] Carlson, L., Fitzgerald, J. & Webster, R., Cathodic protection design for $1,900$ miles (3050 km) of high-pressure natural gas pipeline. *Materials Performance*, **40(8)**, pp. 28–32, 2001.